Article

Thermoeconomic Optimization of a Polygeneration System Based on a Solar-Assisted Desiccant Cooling

Luis Gabriel Gesteira [1,2,*], Javier Uche [2], Francesco Liberato Cappiello [3] and Luca Cimmino [3]

1   Department of Mechanical Technology, Federal Institute of Bahia, Salvador 40301-015, Brazil
2   CIRCE Research Institute, University of Zaragoza, 50018 Zaragoza, Spain
3   Department of Industrial Engineering, University of Naples Federico II, P.le Tecchio 80, 80138 Naples, Italy
*   Correspondence: 773948@unizar.es

Abstract: This paper presents a thermoeconomic analysis of a polygeneration system based on solar-assisted desiccant cooling. The overall plant layout supplies electricity, space heating and cooling, domestic hot water, and freshwater for a residential building. The system combines photovoltaic/thermal collectors, photovoltaic panels, and a biomass boiler coupled with reverse osmosis and desiccant air conditioning. The plant was modeled in TRNSYS and simulated for 1 year. A parametric study defined the system's setup. A thermoeconomic optimization determined the set of parameters that minimize the simple payback period. The optimal structure showed a total energy efficiency of 0.49 for the solar collectors and 0.16 for the solar panels. The coefficient of performance of the desiccant air conditioning was 0.37. Finally, a sensitivity analysis analyzed the influence of purchase electricity and natural gas costs and the electricity sell-back price on the system. The optimum simple payback was 20.68 years; however, the increase in the energy cost can reduce it by up to 85%.

Keywords: renewable energy; building; polygeneration system; desiccant air conditioning; optimization

1. Introduction

In the last 20 years, climate change has become a relevant issue in the global scenario [1]. As a matter of fact, the global average temperature is constantly increasing, and the effects of greenhouse gas (GHG) emissions in the atmosphere are dramatic [2]. EU countries have established several strategies to face the climate change issue by increasing the usage of renewables in their systems [3]. The ever-increasing primary energy consumption in all the energy sectors has led to the necessity of exploiting alternative renewable sources [4]. Polygeneration systems based on renewable energy sources (RESs) can replace traditional machinery and supply several energy demands, consequently reducing CO_2 emissions and increasing primary energy saving, as renewables are renewed by the environment and release little or even no carbon dioxide [5]. The concept of the polygeneration system is to exploit one or more renewable sources to simultaneously provide electricity, heating, cooling, and fuels [6]. In the case of residential applications, instead of producing fuels, these systems are used to produce freshwater [7]. The adoption of innovative renewable-based systems for residential applications is becoming increasingly proposed in the scientific literature [8]. Moreover, the study of innovative control strategies to optimize building heating and cooling systems performances is increasingly developing [9].

Several technologies may be adopted for polygeneration systems, based on the different energy source that is supposed to be exploited [10]. The most commonly adopted source in the case of residential applications is the solar one. In recent work, Alqaed et al. [11] proposed a comparative analysis of three polygeneration systems combining in different configurations a desiccant cooling system, an organic Rankine cycle, and a humidification–dehumidification desalination device. N-octane was used as an organic fluid for the ORC

cycle. Results for the optimal configuration showed a production of 102 kW for electricity (all systems), 214.7 kg/h of freshwater (System 2), 29.94 kW of heating (System 2), 225.6 kW of cooling (System 1), and an overall energy efficiency of 0.6303 (System 1). In a more recent study [12], the n-octane solution was compared with other organic fluids such as R245fa, R113, isopentane, and toluene. R113 showed the best result in terms of the energy efficiency of the system.

The polygeneration structure can vary widely to be suitable for different types of buildings and be assessed based on three main indicators, i.e., technical, economic, and environmental [13]. In particular, Chabaud et al. [14] evaluated a novel energy resource management approach in a residential microgrid, using energy and economic criteria. A grid-connected building equipped with energy production and storage systems was modeled and simulated. The authors outlined that the combination of photovoltaic (PV) and wind turbine (WT) systems is an interesting energy mix option for residential buildings. Figaj et al. [15] investigated the energy performance and economic feasibility of polygeneration systems based on biomass, wind turbine, and solar energy for small isolated districts. The polygeneration system also includes thermal and electrical energy storage, an adsorption chiller, and a reverse-osmosis water desalination unit. The proposed system is modeled and simulated through TRNSYS software to dynamically analyze space heating and cooling, electrical energy, and fresh and domestic hot water demands of 10 households located on Pantelleria Island, Italy. Economic results showed that without considering any incentive fee, the simple payback (SPB) of the system proposed ranges between 7 and 12 years. Ceglia et al. [16] recently presented an environmental, energy, and economic analysis of a polygeneration plant based on a geothermal source for district heating and cooling. The residential district is located in Naples, Italy, and the dynamic energy demand is simulated in TRNSYS. Parametric analyses were performed by ranging the depth of the geothermal well and the usage time of the district. The SPB and the net present value are 7 years and EUR 6.11 M, respectively. From the energy point of view, the yearly saved primary energy is 27.2 GWh, with 5490 tons of carbon dioxide emissions avoided.

Buonomano et al. [17] showed a thermoeconomic analysis of a polygeneration system consisting of PV and WT (190 kW and 10 kW, respectively), connected to an energy storage system (ESS) (400 kWh). The plant was modeled in TRNSYS to maximize economic benefits. It was considered time-dependent tariffs applied to the electricity exchanged with the grid and the possibility to store electricity. Results presented a remarkable reduction in operating costs. Calise et al. [18] investigated a thermoeconomic simulation of a polygeneration plant consisting of a solar-assisted heat pump, photovoltaic/thermal collectors (PVT), an adsorption chiller, and an ESS. The system provides domestic hot water (DHW), space cooling and heating, and electricity. Comodi et al. [19] presented the operational results of a residential microgrid system, consisting of a photovoltaic and solar thermal energy plant, a geothermal heat pump, a tank, and an ESS. The results showed that the self-consumption of photovoltaic energy is maximized by the operation of the ESS, with a reduction of electricity fed back to the grid.

Many of the works presented have been proposed for residential applications in warm countries where the large availability of solar energy allows one to make the polygeneration system more profitable. Many interesting works have been proposed in Spain for polygeneration applied to residential buildings analyzing energy and exergy performances [20]. Sigarchian et al. [21] proposed instead a comparative analysis of polygeneration systems in several weather conditions in Iran to analyze the optimal configuration for each case. The analysis shows that in the case of the coldest climate the CO_2 emissions avoided are by 27%, whereas in the warmest case, this value rises to 41%. Unfortunately, the economic feasibility is still far since incentives are needed from the Government to make the systems proposed profitable.

Solar-based systems, namely PV and PVT, are thus widely exploited as renewable energy technologies for the refurbishment of the residential sector. Because of their relevance in this framework, many experimental studies were recently developed to improve their

performance. Praveenkumar et al. [22] recently proposed an experimental study on the optimization of a PV module employing thermos-electric cooling. According to their study, a reduction of roughly 12 °C of the PV module temperature, from about 45 °C to 33 °C, lead to an increase in the cell efficiency of 5%. The drawback of the system is the higher capital cost of the technology than the conventional one. Conversely, the levelized cost of electricity (LCE) is almost the same, around 0.41 USD/kWh, for 8760 hours/year of functioning. The reason is the high power generated thanks to the increase in performance. Ultimately, the same author proposed a 5E analysis of a PV module cooled using a fanless central processing unit (CPU) heat pipe [23]. In this case, the module temperature reduction is 6.7 °C, with a consequent increase in the average power of 1.66 W. The increase in the electric efficiency is 2.98% for the cooled panel, and the embodied energy recorded is 438.52 kWh. The main findings of the LCE analysis show that in the case of a cooled panel, the cost may range from 0.277 to 0.964 USD/kWh, depending on the hours of functioning. Results for the uncooled panel are close, with an LCE from 0.205 to 0.698 USD/kWh, confirming the relevance of the results obtained.

Furthermore, optimization techniques can be used in polygeneration systems to find their best configuration or to improve performance parameters. Stadler et al. [24] examined 139 different commercial buildings in California, performing an analysis of the economic and environmental benefits. A mixed-integer linear algorithm was developed to evaluate the building energy costs and CO_2 emissions. Singh et al. [25] built up a PV–wind system, including biomass and electrical storage. The system matched the electrical load demand of a small-scale zone. In the work, the ideal sizing of components was defined through an artificial bee colony and particle swarm algorithms. The results highlighted the robustness of the algorithm in terms of good-quality results. Destro et al. [26] investigated the ideal design and management strategy of a trigeneration plant for an isolated hotel in the North of Italy consisting of a PV field, a thermal energy storage (TES), a diesel combined heat and power (CHP) engine, and two ESSs, namely, a pumped hydro and a lead–acid battery. The configuration and operation strategies were defined by applying a particle swarm optimization algorithm to reduce costs and meet the hotel's consumption of electricity, heating, cooling, and freshwater.

A large number of papers present polygeneration schemes for cooling, heating, electricity, DHW, and desalinated water production. However, to the best of the authors' knowledge, none of the papers already published include a detailed dynamic thermoeconomic optimization of a polygeneration system based on a solar-assisted desiccant air conditioning (DAC) to supply five demands for the residential sector. To cover such a lack of literature, the present study aims to perform a Hooke–Jeeves optimization to minimize the SPB of a polygeneration system. Furthermore, a sensitivity analysis was performed to investigate the system's behavior according to the electricity and natural gas prices.

2. Materials and Methods

2.1. System Layout

The system's layout is presented in Figure 1. The plant attends to a domestic dwelling. It consists of PVT collectors, PV panels, and a biomass boiler (BB) for electricity and heating production, as well as reverse osmosis (RO) for potable water and DHW demands and a DAC for cooling. Extra devices were used, and all parameters were accurately selected to allow the system proper operation.

The proposed system (PS) is an improvement of the polygeneration plant reported by Gesteira et al. [27]. Here, PV panels, a BB, and a second TES were added to increase the system's robustness. Solar energy is converted into electricity and heat through PV panels and PVT collectors. The best irradiation yield was found for a slope of 35° for the city. The demand of electricity includes all power loads and the building's consumption. The PV panels and PVT collectors are connected to an inverter with peak-power tracking. It allows electricity purchase and sale back to the utility. The grid behaves as a backup as

the solar energy is intermittent, and there is a non-simultaneity between generation and demand [28].
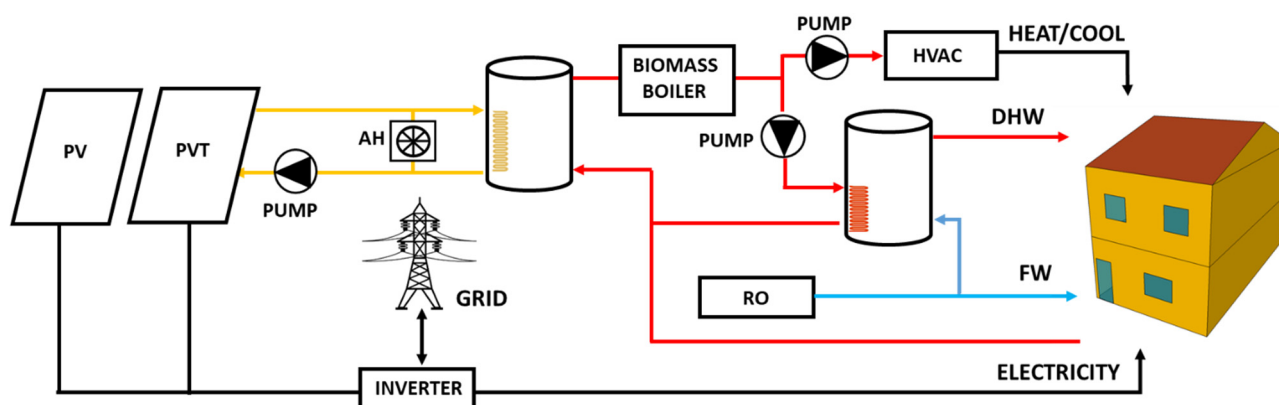

Figure 1. Polygeneration system layout.

A primary TES is used to mitigate the intermittence of solar radiation and a secondary TES supplies DHW for the residence on demand. Moreover, an air heater (AH) dissipates heat whenever the PVT's outlet temperature increases over 100 °C. The primary TES works as a preheater for the boiler, which feeds the heating, ventilation, and air conditioning (HVAC) system, and the secondary TES. The HVAC system supplies heating in the winter season and cooling in the summer. In the winter period, the thermal energy is directly exploited for building space heating. On the other hand, during summer, a DAC system consumes thermal energy to supply building space cooling. Moreover, a tempering valve merges the water heated in the secondary TES with the freshwater and supplies DHW at 45 °C.

2.2. System Model

The PS was modeled in the TRNSYS simulation studio (version 18) [29]. Most of the components come from the software's built-in library. However, some of them are user-defined. A detailed description of the component models used in the simulation is available in TRNSYS's component mathematical reference. In this section, a detailed description of the PV panels and the inverter models are reported. The user-defined and manufacturer's technical data of the PV panels are presented in Table 1.

Table 1. Main parameters of the PV panels.

Component	Parameter	Symbol	Value	Unit
	Slope	θ_S	35	°
	Azimuth	θ_A	0	°
	Module area	A_{PV}	1.93	m^2
	Short-circuit current at reference conditions	$I_{sc,ref}$	9.38	A
	Open-circuit voltage at reference conditions	$V_{oc,ref}$	46.2	V
PV	Reference cell temperature	$T_{c,ref}$	25	°C
	Reference insolation	$G_{T,ref}$	1	kW/m^2
	Voltage at max power point and reference conditions	$V_{mp,ref}$	37.5	V
	Current at max power point and reference conditions	$I_{mp,ref}$	8.81	A
	Temperature coefficient of Isc at reference condition	μ_{Isc}	0.0032	1/°C
	Temperature coefficient of Voc at reference condition	μ_{voc}	25	°C
	Module temperature at NOCT	$T_{c,NOCT}$	45	°C

2.2.1. PV Panel Model

The PV model (Type 103) is a polycrystalline photovoltaic panel. The array works through a maximum power point tracker. The model is based on the "four parameters"

model based on the manufacturers' data for generating an IV curve at each time step [30,31]. The first parameter is the $I_{L,ref}$, which is the photocurrent at reference condition; the second one is the $I_{0,ref}$, which is the diode reverse saturation current at reference condition; γ is the third parameter and means the empirical PV curve-fitting and finally the R_s, which is the module series resistance [32]. The IV curve slope at the short-circuit condition is null. The current-voltage equation of the circuit is shown in Equation (1):

$$I = I_{L,ref} \frac{G_T}{G_{T,ref}} - I_{o,ref} \left(\frac{T_c}{T_{c,ref}} \right)^3 \left[\exp \left(\frac{q}{\gamma k T_c} (V + I R_s) \right) - 1 \right] \tag{1}$$

The current (I_{mp}) and the voltage (V_{mp}) at the maximum power point are analyzed using an iterative process. Algorithms are used to solve the four equivalent circuit characteristics. Firstly, the voltage and current are replaced in Equation (1) at the short-circuit, open-circuit, and maximum power conditions. Then by considering a rearrangement the following Equations (2)–(4) are obtained depending on $I_{L,ref}$, γ, and $I_{0,ref}$:

$$I_{L,ref} \approx I_{sc,ref} \tag{2}$$

$$\gamma = \frac{q \left(V_{mp,ref} - V_{oc,ref} + I_{mp,ref} R_s \right)}{k T_{c,ref} \ln \left(1 - \frac{I_{mp,ref}}{I_{sc,ref}} \right)} \tag{3}$$

$$I_{o,ref} = I_{sc,ref} \exp^{-\left(\frac{q V_{oc,ref}}{\gamma k T_{c,ref}} \right)} \tag{4}$$

The last unknown parameter needs another equation to be determined, i.e., the analytical derivative of voltage:

$$\frac{\partial V_{oc}}{\partial T_c} = \mu_{voc} = \frac{\gamma k}{q} \left[\ln \left(\frac{I_{sc,ref}}{I_{o,ref}} \right) + \frac{T_c \mu_{isc}}{I_{sc,ref}} - \left(3 + q \varepsilon \left(\frac{\gamma}{N_s} k T_{c,ref} \right)^{-1} \right) \right] \tag{5}$$

N_s is the number of cells in the module, q is the constant of the electron charge, k is the Boltzmann constant, and ε is the bandgap of the semiconductor.

2.2.2. Inverter Model

The inverter (Type 48) is a peak-power tracking device, with no battery as backup. The inverter converts the DC power to AC and sends it to the load and/or to the utility. It allows the power purchase or sale back with the grid. When the production is higher than the consumption, the excess is sent to the utility. When the production is not sufficient to meet the consumption, the power is taken from the utility.

2.2.3. Energy Model

Primary energy saving (PES) analyzes the energy performance of the PS. A reference system (RS) supposes all demands produced by conventional technologies. The assumptions considered were a national grid efficiency (η_{el}) of 0.42 [33] and a natural gas boiler efficiency (η_{th}) of 0.92 [34]. A cooling coefficient of performance based on an electric chiller (COP_{ECH}) of 2.6 [34]. Freshwater is fully provided by the RO unit powered by the national grid, as it is considered a coastal area with water scarcity. Thus, electricity consumption aggregates freshwater demand.

The PES and its ratio (PES_R) are calculated as shown in Equations (6) and (7):

$$PES = PE_{RS} - PE_{PS} \tag{6}$$

$$PES_R = \frac{PES}{PE_{RS}} \tag{7}$$

$$PE_{RS} = \left(\frac{P_{el,dem}}{\eta_{el}} + \frac{Q_{DHW,dem} + Q_{heat,dem}}{\eta_{th}} + \frac{Q_{cool,dem}}{COP_{ECH} \cdot \eta_{el}} \right)_{RS} \tag{8}$$

$$PE_{PS} = \left(\frac{P_{grid,aux}}{\eta_{el}} + \frac{Q_{DHW,aux} + Q_{heat,aux}}{\eta_{th}} + \frac{Q_{cool,aux}}{COP_{ECH} \cdot \eta_{el}} \right)_{PS} \tag{9}$$

$P_{grid,aux}$ is the electricity taken from the utility to match PS consumption, and $Q_{DHW,aux}$, $Q_{heat,aux}$, and $Q_{cool,aux}$ are the thermal need to be provided by a gas boiler (GB) for DHW and space heating, and by an electric chiller (ECH) for space cooling, respectively.

2.2.4. Environmental Model

Following the same approach, the environmental analysis is presented by the CO_2 saving as displayed in Equations (10) and (11):

$$CO_2 = CO_{2RS} - CO_{2PS} \tag{10}$$

$$CO_{2R} = \frac{CO_2}{CO_{2RS}} \tag{11}$$

$$CO_{2RS} = \left(P_{el,dem} + \frac{Q_{cool,dem}}{COP_{ECH}} \right) \cdot f_{CO_2,EE} + \frac{Q_{DHW,dem} + Q_{heat,dem}}{\eta_{th}} \cdot f_{CO_2,NG} \tag{12}$$

$$CO_{2PS} = \left(P_{grid,aux} + \frac{Q_{cool,aux}}{COP_{ECH}} \right) \cdot f_{CO_2,EE} + \frac{Q_{DHW,aux} + Q_{heat,aux}}{\eta_{th}} \cdot f_{CO_2,NG} \tag{13}$$

The CO_2 emission factor of natural gas usage $f_{CO_2,NG}$ in Spain is 0.204 kgCO_2/kWh [35]. The emission factor associated with the Spanish national grid $f_{CO_2,EE}$ is 0.19 kgCO_2/kWh [36].

2.2.5. Economic Model

In this section, a detailed economic analysis is presented to assess the economic feasibility of the polygeneration plant. The operating cost of all components was estimated. Cost functions were introduced to calculate the capital costs of the PS. In particular, the PVT capital cost, Equation (14), is computed as a function of the solar field area A_{PVT} [37]:

$$C_{PVT} = 200 \cdot A_{PVT} \tag{14}$$

The PV unit capital cost per kW, Equation (15), is defined as [38]:

$$CPV = 1000 \text{ EUR/kW} \tag{15}$$

The thermal storage cost, Equation (16), is obtained as a function of its volume, V_{TK} [39]:

$$C_{TK} = 494.9 + 808.0 \cdot V_{TK} \tag{16}$$

The capital cost of the inverter C_{inv} is calculated as a function of the nominal power of the PVT collectors and PV panels (P_{PVT}, P_{PV}) assuming a specific cost equal to 180 EUR/kW$_{el}$ [17]:

$$C_{inv} = 180 \cdot (P_{PVT} + P_{PV}) \tag{17}$$

The biomass boiler capital cost, C_{boiler}, is estimated by IDAE [40] as:

$$C_{boiler} = 282 \text{ EUR/kW} \tag{18}$$

RO device cost C_{RO} was taken from the TRHIBERDE project reported by Acevedo et al. [41]:

$$C_{RO} = \text{EUR } 4650 \tag{19}$$

Regarding the DAC cost, it is a heat-driven component and an effective air conditioner for residential buildings in regions where the use of thermal energy is more economical than electrical power, or when thermal energy is available, i.e., coming from solar collectors. The cost of a desiccant-based air handling unit was presented by Angrisani et al. [42]. Its

specific investment cost C_{DAC} related to the nominal cooling capacity of the system was also reported by the same author [43]:

$$C_{DAC} = 1090 \text{ EUR/kW}_{th} \tag{20}$$

Finally, the cost of the pumps was reported by Buonomano et al. [44]:

$$C_{pump} = 1.08 \cdot \left(-0.00000002 \cdot Q_{pump}^2 + 0.0285 \cdot Q_{pump} + 388.14 \right) \tag{21}$$

For the cost of all other components required in the system (pipes, valves, controllers, etc.), 20% of the capital cost was assumed. Thus, the total capital cost of the PS was estimated as:

$$C_{PS,tot} = 1.2 \cdot \left(C_{PVT} + C_{PV} + C_{TK} + C_I + C_{boiler} + C_{DAC} + C_{RO} + C_{pump} \right) \tag{22}$$

In addition, the PVT maintenance yearly cost is estimated equal to 2% of the capital cost of the PVT field [37]:

$$M_{PVT} = 2\% \cdot C_{PVT} \tag{23}$$

A PV maintenance annual cost is equal to [38]:

$$M_{PV} = 1\% \cdot C_{PV} \tag{24}$$

A RO unit maintenance cost is estimated as 1.5% of its capital cost [45]:

$$M_{RO} = 1.5\% \cdot C_{RO} \tag{25}$$

Regarding the operating cost of the biomass boiler, a maintenance cost is estimated as 1% of the boiler investment cost [46]:

$$M_{boiler} = 1\% \cdot C_{Boiler} \tag{26}$$

DAC systems are very reliable, so their maintenance cost was neglected.

The economic yearly saving of the PS considers the economic profits with respect to the RS. In the RS, the national utility provides electricity. Conversely, in the PS, the PV panels, the PVT collectors, and the grid match the electric user load. Moreover, the PS is allowed to sell back electricity to the utility at 80% of the purchase price. Considering time-dependent tariffs, the electricity is withdrawn from the national grid with a cost, c_{el}, composed of a fixed, $c_{el,fix}$, and a variable, $c_{el,var}$, parts. $c_{el,fix}$ is proportional to the contracted power, and it is considered in both RS and PS systems; thus, it can be negligible. Conversely, the $c_{el,var}$ is calculated based on the electricity consumption. Values of purchased electricity in EUR/kWh depend on time-of-use tariff are shown in Table 2 [35].

Table 2. Electricity tariffs in Spain.

Period	Hours	$c_{el,fix}$ (EUR/kWy)	$c_{el,var}$ (EUR/kWh)
P1	14–23		0.173941
P2	1, 8–13, 24	47.816	0.099554
P3	2–7		0.076838

In the case of natural gas costs, c_{ng}, the contract depends on the annual gas consumption, which is related to a fixed cost, $c_{ng,fix}$. The variable cost of natural gas, $c_{ng,var}$, is proportional to its usage (Table 3) [35].

Table 3. Natural gas tariff in Spain.

$c_{ng,fix}$ (EUR/y)	$c_{ng,var}$ (EUR/kWh)
61.8	0.063125

Regarding the tap water cost, c_w, in Mediterranean cities, a unit cost of 2 EUR/Sm^3 was considered [47]. Furthermore, for the biomass boiler operation, a biomass (wood-chip) cost, c_b, was reported by IDEA [40] as 0.193 EUR/kg with a Lower Heating Value (LHV) set to 5.2 kWh/kg and a combustion efficiency of 0.85 [46].

So, the annual savings of the PS concerning the RS were calculated as:

$$J_{tot} = C_{op,RS} - C_{op,PS} \tag{27}$$

$$C_{op,RS} = \left(P_{el,dem} + \frac{Q_{cool,dem}}{COP_{ECH}} \right) \cdot c_{el,var} + \frac{Q_{DHW,dem} + Q_{heat,dem}}{\eta_{th}} \cdot c_{ng,var} + c_{ng,fix} + FW_{dem} \cdot c_w \tag{28}$$

$$C_{op,PS} = \left(P_{el,purc} - P_{el,sold} \right) \cdot c_{el,var} + \frac{Q_{boiler}}{\eta_{th} \cdot LHV_b} \cdot c_b + M_{PVT} + M_{PV} + M_{RO} + M_{boiler} \tag{29}$$

Finally, the economic performance of the PS was evaluated by the SPB, Equation (22), calculated as the ratio of the total capital cost and the savings obtained by PS. A lifetime of 20 years for the entire system was assumed, except for the inverter and the RO unit, for which 10 years was considered [18,45].

$$SPB = \frac{J_{tot}}{Cop, RS - Cop, PS} \tag{30}$$

In this study, the annual savings are assumed to be constant over the 20 years life span. In other words, it is assumed that electricity costs remain unchanged and that PV and PVT degradation are neglected. Similarly, it is also assumed that the solar radiation profile is the same for all periods. Therefore, in this work, the cash flow is developed considering an annual cost-saving constant over the system's lifetime.

3. Results

The case study is reported by Gesteira et al. [48]. It consists of a single family dwelling based in Almería, Spain. Meteonorm weather data for Almería (36°50'17" N, 2°27'35" W) were used during the simulation. It is worth noting that polygeneration systems applied to European Mediterranean countries can reach up to 80% of energy savings with a suitable level of energy mixture [49]. Figure 2 displays the building's 3D view and its floor plan.
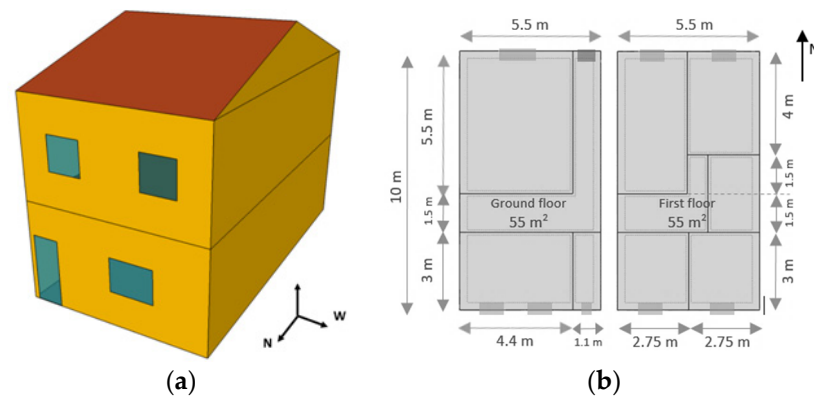

(a)   (b)

Figure 2. Building geometrical (**a**) and architectural models (**b**).

The simulation was performed from 0 h to 8760 h (1 year) with a 5 min time step. Firstly, to investigate the system's best configuration, a parametric study was carried out. Then, a thermoeconomic optimization was used to determine the set of parameters that minimize the simple payback period. For that reason, the number of PV panels, PVT collectors, and primary and secondary TES volumes was optimized. The yearly results of the optimal structure are presented for the main parameters. Finally, a sensitivity analysis was performed to investigate the system's behavior according to the electricity and natural gas prices.

3.1. Parametric Study

A parametric study was carried out to investigate the most significant design variables when all other parameters remain fixed. The top temperature of the secondary TES ($T_{TES2,top}$) and the boiler outlet temperature ($T_{boiler,out}$) were analyzed as they affect the thermal demand coverages. Furthermore, the study was also performed to define the minimum boiler power capacity (P_{boiler}). $T_{TES2,top}$ and $T_{boiler,out}$ were both varied from 45 °C to 55 °C, while P_{boiler} ranged from 8 to 20 kW.

3.1.1. Parametric Study: Secondary TES Top Temperature

Increasing the $T_{TES2,top}$ leads to an increase in the DHW coverage, as this temperature ensures the achievement of the hot water setpoint defined for the house. As seen in Figure 3, the coverage is almost constant for $T_{TES2,top}$ higher than 49 °C. Thus, it is not convenient to increase $T_{TES2,top}$ over 49 °C, as the maximum DHW coverage is already achieved.
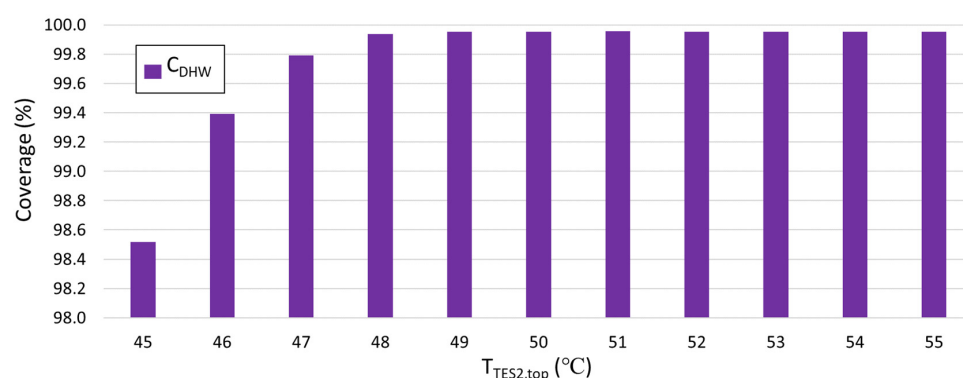

Figure 3. Domestic hot water coverage, the top temperature of the secondary TES.

3.1.2. Parametric Study: Boiler Outlet Temperature

The boiler outlet temperature affects all thermal demands. The minimum $T_{boiler,out}$ is equal to $T_{TES2,top}$, which was already defined in the previous analysis. $T_{TES2,top}$ of 49 °C ensures the maximum DHW coverage. However, the maximum HVAC coverage was not achieved yet. The increase in the $T_{boiler,out}$ provides a higher temperature for the heating fan coil and the DAC regenerator. Figure 4 shows that the coverages are directly proportional to the boiler outlet temperature. The heating and cooling coverages increased from 96% to 102% and from 97% to 104%, respectively. Therefore, there is no energy convenience to increase $T_{boiler,out}$ to values higher than 51 °C. This temperature was selected as a setpoint for the boiler as it provided the maximum coverage for both cooling and heating demands.
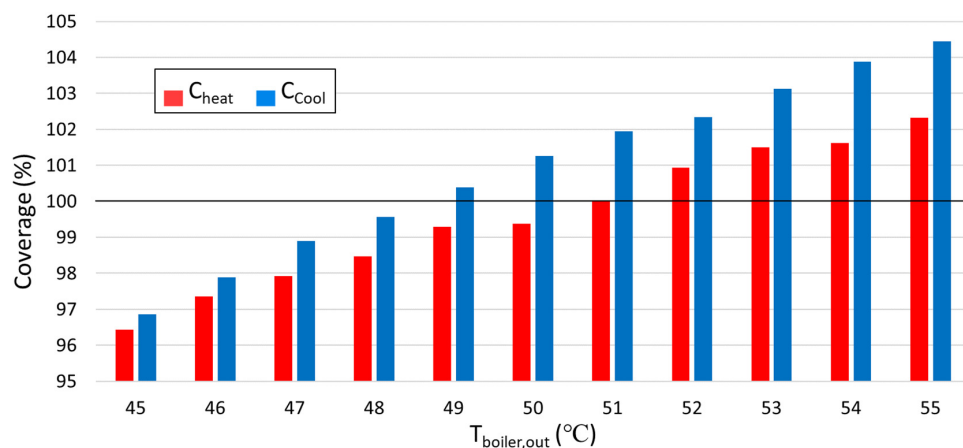

Figure 4. Cooling and heating coverages, boiler outlet temperature.

3.1.3. Parametric Study: Boiler Power Capacity

The BB adds heat to the flow stream at its power capacity (P_{boiler}) whenever the boiler outlet temperature ($T_{boiler,out}$) is less than a setpoint. It performs like an auxiliary heater with an internal control to maintain $T_{boiler,out}$ fixed. The boiler power is related to the capacity of providing an outlet temperature whenever it is required during the simulation. The minimum power capacity commercially available was considered 8 kW. Figure 5 shows the correlation between the P_{boiler} and the thermal coverages. The DHW coverage can be satisfied for all capacities due to its lower temperature requirement. Lower power capacities affect cooling, which achieves 100% at 9 kW. Heating shows the same trend as the others' demands; however, it only meets full coverage at 12 kW. Thus, the power capacity of 12 kW was selected for the boiler as it provided 100% coverage for all house thermal demands.
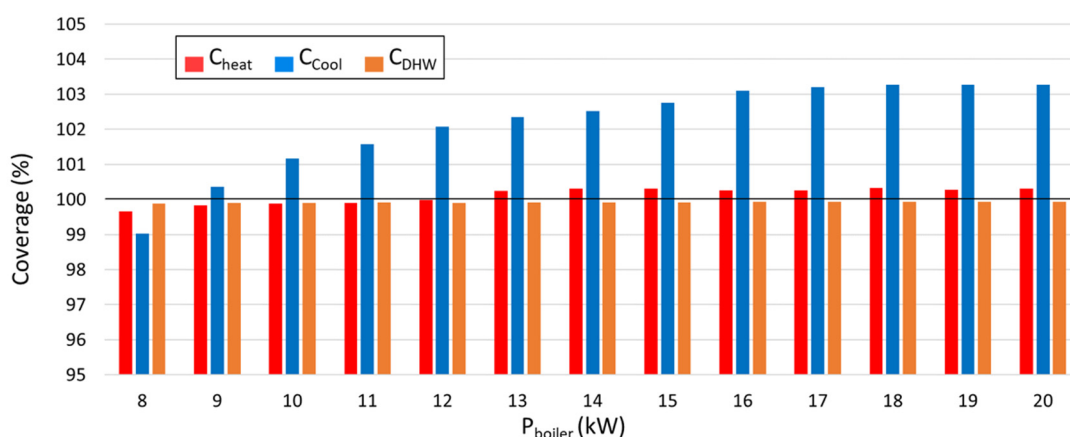

Figure 5. Heating, cooling, and DHW coverages, boiler power capacity.

3.2. Thermoeconomic Optimization

A thermoeconomic optimization was implemented using the TRNOPT tool included in the TRNSYS simulation studio. TRNOPT is designed to link the optimization algorithm and the dynamic simulation. A complex mathematical algorithm is performed by the GENOPT package developed by Lawrence Berkeley National Laboratory [50]. In particular, the Generalized Search Method was used in the optimization by the Hooke–Jeeves [51] modified algorithm. The optimization was performed considering the main design variables, namely: the number of PVT collectors (N_{coll}), number of PV panels (N_{pan}), primary TES volume (V_{TES1}), and secondary TES volume (V_{TES2}). Moreover, the SPB was selected as the optimization objective function. Table 4 shows the details of the main variables. The optimization range is defined by its minimum and maximum values. The first attempt starts with the initial value and proceeds with the iterations according to the step size.

Table 4. Optimization variables breakdown.

Variables	Ncoll	Npan	V_{TES1}	V_{TES2}
Initial Value	15	15	2.5	0.15
Minimum Value	1	1	0.3	0.05
Maximum Value	30	25	5	0.3
Step Size	1	1	0.1	0.05

Figure 6 shows the SPB and the design variables as a function of the optimization iteration. The optimization process converged in a bit over 150 iterations. The optimal configuration is obtained when the SPB achieves its minimum value. The optimum SPB value of 20.68 years was obtained for 9 PVT collectors, 25 PV panels, and a primary and secondary TES volume of 1.35 m^3 and 0.25 m^3, respectively. Moreover, it is worth noting

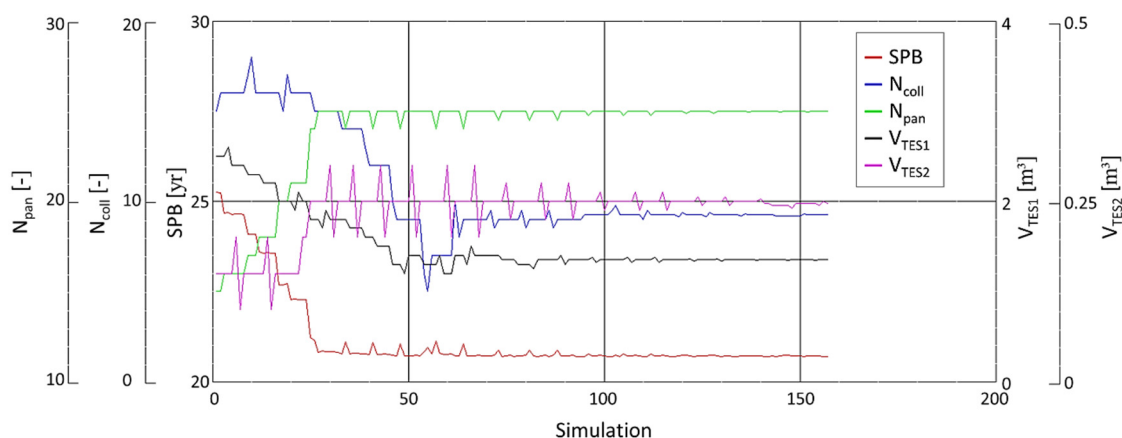that the number of collectors and panels was limited to 50 m^2 due to the available roof area at the house.

Figure 6. SPB and the design variables, optimization iteration.

3.3. Yearly Results

The annual results for the optimal solution are summarized in Table 5. The table presents the yearly integrated number of electricity, heat, and water volume. Moreover, the performance parameters are also presented. The building demands were taken from Ref. [48].

Table 5. Yearly results.

Parameter	Symbol	Value	Unit
Freshwater demand	$m_{FW,dem}$	151	m^3/yr
Electricity demand	$P_{el,dem}$	5.11	MWh/yr
DHW demand	$Q_{DHW,dem}$	1.26	MWh/yr
Cooling demand	$Q_{cool,dem}$	1.45	MWh/yr
Heating demand	$Q_{heat,dem}$	0.94	MWh/yr
RO freshwater production	m_{RO}	151	m^3/yr
PV power production	P_{PV}	16.81	MWh/yr
PVT power production	P_{PVT}	2.91	MWh/yr
Power loss	P_{loss}	1.97	MWh/yr
Total power production	$P_{tot,prod}$	17.75	MWh/yr
PVT heat production	Q_{PVT}	9.53	MWh/yr
Biomass boiler production	Q_{boiler}	1.54	MWh/yr
Air heater dissipation	Q_{AH}	1.18	MWh/yr
Heat loss	Q_{loss}	3.13	MWh/yr
Total useful heat production	$Q_{tot,prod}$	6.75	MWh/yr
PV efficiency	η_{PV}	0.16	–
PVT efficiency	η_{PVT}	0.49	–
DAC thermal COP	COP_{DAC}	0.37	–
Primary energy saving	PES	12.9	MWh
CO$_2$ saving	CO$_2$	1.29	tonCO$_2$
Simple payback	SPB	20.69	yr

The power generation ($P_{tot,prod}$) is the PV (P_{PV}) and PVT (P_{PVT}) generation minus the losses (P_{loss}) due to the inverter's inefficiency (10%). The excess power is injected into the grid (12.64 MWh/yr).

The total useful heat production ($Q_{tot,prod}$) is the PVT heat generation (Q_{PVT}) and the BB production (Q_{boiler}) subtracted by the energy released by the AH (Q_{AH}) and the total energy dissipated to the surroundings (Q_{loss}). The heat released by the AH is about

12% of Q_{PVT}. Moreover, $Q_{tot,prod}$ is used for attending $Q_{DHW,dem}$, $Q_{heat,dem}$, and $Q_{cool,dem}$; however, as the DAC thermal COP is equal to 0.37, the heat requested by the regenerator was 4.43 MWh/yr.

3.4. Sensitivity Analysis

A sensitivity analysis investigated how electricity purchase, electricity sell-back, and natural gas prices affect the economic performance of the PS. Thus, the purchasing costs were progressively increased, and the sell-back price was reduced (Table 6). Each parameter was evaluated for each case, and the optimization results were collected.

Table 6. Sensitivity analysis variables.

Parameter	Case 1	Case 2	Case 3	Case 4	Case 5
Electricity purchase cost	+50%	+100%	+150%	+200%	+250%
Natural gas purchase cost	+50%	+100%	+150%	+200%	+250%
Electricity sell-back cost	−10%	−20%	−30%	−40%	−50%

3.4.1. Sensitivity Analysis: Purchase Cost of Electricity

Considering that the RS is based on the consumption of electricity, the increase in the energy price worsens economic performance. Conversely, in the PS, electricity may be sold back to the grid. Thus, higher energy cost enhances its economic performance because the sell-back cost of electricity is a ratio of the electricity purchase cost. The increase in the electricity cost leads to an increase in the operational cost of the RS and improves the economic savings of the PS. Figure 7 displays the sensitivity analysis of the electricity purchase cost.
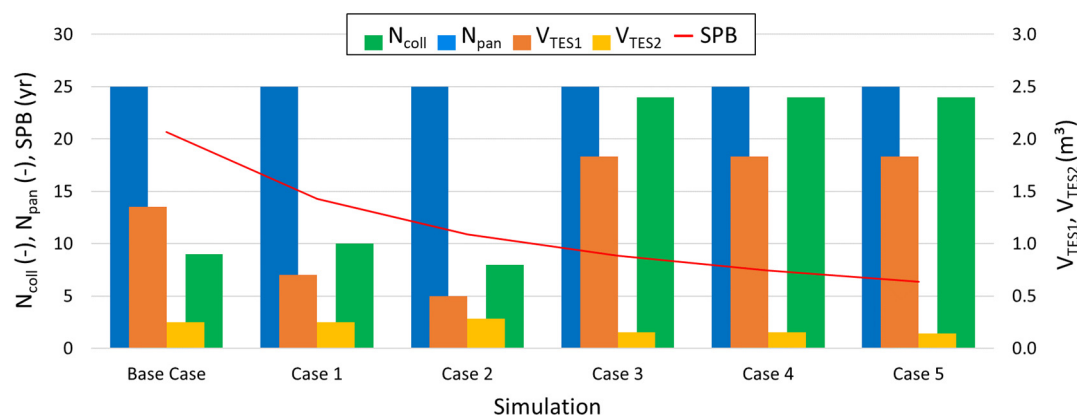

Figure 7. SPB and the design variables, optimization case (purchase cost of electricity).

The number of PV panels remains constant at 25 for all cases simulated. The number of PVT collectors increases from 9 to 24 between the second and third cases. At the same point, the volume of the primary TES increases, following the higher thermal energy availability, and the secondary TES volume decreases. It demonstrates that as of Case 3, the energy cost becomes very expensive; thus, the electricity sold back to the grid is more attractive, as it is proportional to the purchase cost. Therefore, electricity production increased to its maximum. The SPB decreases to 6.38 years when the purchase cost of electricity increases up to 250%.

3.4.2. Sensitivity Analysis: Purchase Cost of Natural Gas

The RS is also dependent on natural gas consumption; thus, the increase in the energy price worsens the economic performance. On the other hand, the PS is not affected by the natural gas cost. The increase in the natural gas cost leads solely to an increase in the

operational cost of the RS. Therefore, the SPB decrease is slighter compared to the previous case. Figure 8 displays the sensitivity analysis of the natural gas purchase cost.
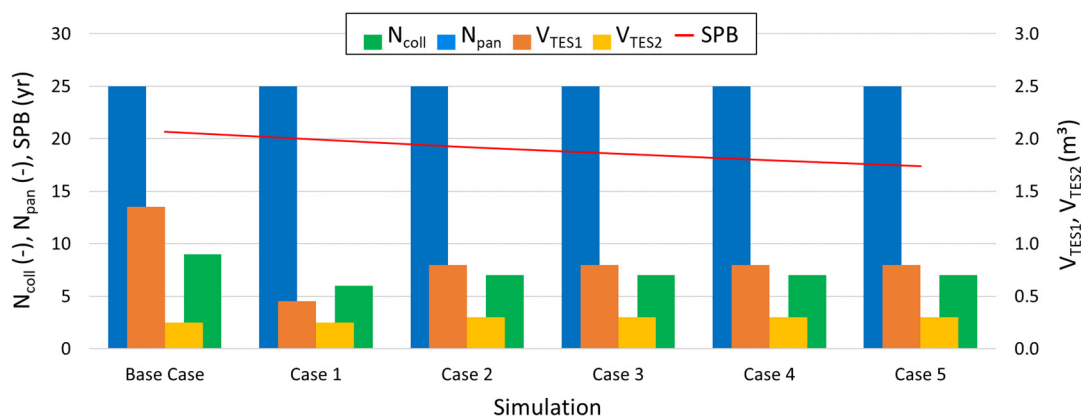

Figure 8. SPB and the design variables, optimization case (purchase cost of natural gas).

The number of PV panels remains constant at 25 for all cases simulated. The number of PVT collectors and the primary and secondary TES volumes present a minor variation around 7, 0.8 m^3, and 0.3 m^3, respectively. The SPB decreases 15.81% from the base case to the last case, while the purchase cost of natural gas increases up to 250%.

3.4.3. Sensitivity Analysis: Sell-Back Cost of Electricity

In the PS, electricity may be sold back to the grid with a price defined as a ratio of the electricity purchase cost. Thus, a lower sell-back cost worsens its economic performance. The decrease in this ratio leads to an increase in the operational cost of the PS. Figure 9 displays the sensitivity analysis of the sell-back cost of electricity.
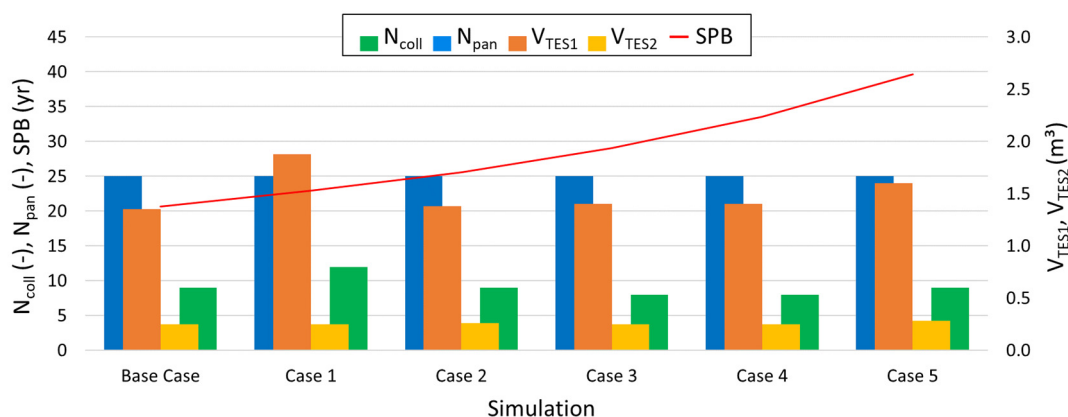

Figure 9. SPB and the design variables, optimization case (sell-back cost of electricity).

Again, the number of PV panels remains constant at 25 for all cases simulated. The number of PVT collectors and primary and secondary TES varies between 8 to 12, 1.35 to 1.88 m^3, and 0.25 to 0.28 m^3, respectively. It indicates that the system design is relatively constant along the iterations. However, the SPB increases to 39.61 years when the sell-back cost of electricity decreases to 30% of the purchase cost.

4. Conclusions

This study performed a thermoeconomic analysis of a solar-assisted desiccant cooling polygeneration plant. The facility provides electricity, space heating and cooling, DHW, and potable water for a residential building. The system combines photovoltaic/thermal collectors, photovoltaic panels, and a biomass boiler coupled with reverse osmosis and

desiccant air conditioning. The plant was applied to a dwelling for a Spanish single family. The system's model was performed in the TRNSYS simulation studio. A parametric study, a thermoeconomic optimization, and a sensitivity analysis of the system were performed. The main findings are summarized below:

1. The top temperature of the secondary TES and the boiler outlet temperature and power capacity were defined as 49 °C, 51 °C, and 12 kW, respectively.
2. The optimum SPB value of 20.68 years was obtained for 9 PVT collectors, 25 PV panels, and a primary and secondary TES volume of 1.35 m^3 and 0.25 m^3, respectively.
3. The optimal structure showed a total energy efficiency of 0.49 for the solar collectors, 0.16 for the solar panels, and a desiccant air conditioning coefficient of performance of 0.37
4. The yearly results showed that 12.64 MWh/yr of electricity was injected into the grid.
5. The increase in the electricity purchase cost makes the proposed polygeneration system economically profitable. On the other hand, the decrease in the electricity sell-back cost reduces its feasibility. The increase in the natural gas cost is not very relevant to the system's profitability decision making.
6. The highest prices of electricity and natural gas (+250%) and the sell-back cost of electricity (base case) can reduce the SPB by up to 85%.

Regarding the system, variations in solar energy can be found over the 20-year life span. Moreover, the time-dependent tariff may vary year by year due to inflation or energy scarcity periods. However, it is impossible to predict the behavior of climate conditions and the future time-dependent prices of electricity over such a long period. Furthermore, PV and PVT degradation may be neglected (around 1% per year). Finally, the system may be a good solution for matching the energy consumption using renewables mostly if a capital investment subsidy is considered.

Author Contributions: Conceptualization, J.U.; methodology, F.L.C., L.C. and L.G.G.; formal analysis, L.G.G.; investigation, L.C. and L.G.G.; resources, J.U.; data curation, F.L.C. and L.G.G.; writing—original draft preparation, L.C. and L.G.G.; writing—review and editing, F.L.C. and J.U.; supervision, J.U. All authors have read and agreed to the published version of the manuscript.

Institutional Review Board Statement: Not applicable.

Informed Consent Statement: Not applicable.

Data Availability Statement: Not applicable.

Conflicts of Interest: The authors declare no conflict of interest.

References

1. Perkins-Kirkpatrick, S.; Green, D. Chapter 2—Extreme Heat and Climate Change. In *Heat Exposure and Human Health in the Context of Climate Change*; Elsevier: Amsterdam, The Netherlands, 2023; pp. 5–36. ISBN 978-0-12-819080-7.
2. Borie, M.; Mahony, M.; Obermeister, N.; Hulme, M. Knowing like a Global Expert Organization: Comparative Insights from the IPCC and IPBES. *Glob. Environ. Chang.* **2021**, *68*, 102261. [CrossRef]
3. Köhl, M.; Linser, S.; Prins, K.; Talarczyk, A. The EU Climate Package "Fit for 55"—A Double-Edged Sword for Europeans and Their Forests and Timber Industry. *For. Policy Econ.* **2021**, *132*, 102596. [CrossRef]
4. Saint Akadiri, S.; Alola, A.A.; Akadiri, A.C.; Alola, U.V. Renewable Energy Consumption in EU-28 Countries: Policy toward Pollution Mitigation and Economic Sustainability. *Energy Policy* **2019**, *132*, 803–810. [CrossRef]
5. Calise, F.; de Notaristefani di Vastogirardi, G.; Dentice d'Accadia, M.; Vicidomini, M. Simulation of Polygeneration Systems. *Energy* **2018**, *163*, 290–337. [CrossRef]
6. Gimelli, A.; Muccillo, M. Development of a 1 KW Micro-Polygeneration System Fueled by Natural Gas for Single-Family Users. *Energies* **2021**, *14*, 8372. [CrossRef]

7. Khoshgoftar Manesh, M.H.; Mousavi Rabeti, S.A.; Nourpour, M.; Said, Z. Energy, Exergy, Exergoeconomic, and Exergoenvironmental Analysis of an Innovative Solar-Geothermal-Gas Driven Polygeneration System for Combined Power, Hydrogen, Hot Water, and Freshwater Production. *Sustain. Energy Technol. Assess.* **2022**, *51*, 101861. [CrossRef]

8. Calise, F.; Cappiello, F.L.; Cimmino, L.; Dentice d'Accadia, M.; Vicidomini, M. Dynamic Simulation and Thermoeconomic Analysis of a Hybrid Renewable System Based on PV and Fuel Cell Coupled with Hydrogen Storage. *Energies* **2021**, *14*, 7657. [CrossRef]

9. Sawant, P.; Villegas Mier, O.; Schmidt, M.; Pfafferott, J. Demonstration of Optimal Scheduling for a Building Heat Pump System Using Economic-MPC. *Energies* **2021**, *14*, 7953. [CrossRef]

10. Calise, F.; Dentice D'Accadia, M. Simulation of Polygeneration Systems. *Energies* **2016**, *9*, 925. [CrossRef]

11. Alqaed, S.; Fouda, A.; Elattar, H.F.; Mustafa, J.; Almehmadi, F.A.; Refaey, H.A.; Alharthi, M.A. Performance Evaluation of a Solar Heat-Driven Poly-Generation System for Residential Buildings Using Various Arrangements of Heat Recovery Units. *Energies* **2022**, *15*, 8750. [CrossRef]

12. Almehmadi, F.A.; Elattar, H.F.; Fouda, A.; Alqaed, S.; Mustafa, J.; Alharthi, M.A.; Refaey, H.A. Energy Performance Assessment of a Novel Solar Poly-Generation System Using Various ORC Working Fluids in Residential Buildings. *Energies* **2022**, *15*, 8286. [CrossRef]

13. Jana, K.; Ray, A.; Majoumerd, M.M.; Assadi, M.; De, S. Polygeneration as a Future Sustainable Energy Solution—A Comprehensive Review. *Appl. Energy* **2017**, *202*, 88–111. [CrossRef]

14. Chabaud, A.; Eynard, J.; Grieu, S. A New Approach to Energy Resources Management in a Grid-Connected Building Equipped with Energy Production and Storage Systems: A Case Study in the South of France. *Energy Build.* **2015**, *99*, 9–31. [CrossRef]

15. Figaj, R.; Żołądek, M.; Homa, M.; Pałac, A. A Novel Hybrid Polygeneration System Based on Biomass, Wind and Solar Energy for Micro-Scale Isolated Communities. *Energies* **2022**, *15*, 6331. [CrossRef]

16. Ceglia, F.; Macaluso, A.; Marrasso, E.; Roselli, C.; Vanoli, L. Energy, Environmental, and Economic Analyses of Geothermal Polygeneration System Using Dynamic Simulations. *Energies* **2020**, *13*, 4603. [CrossRef]

17. Buonomano, A.; Calise, F.; d'Accadia, M.D.; Vicidomini, M. A Hybrid Renewable System Based on Wind and Solar Energy Coupled with an Electrical Storage: Dynamic Simulation and Economic Assessment. *Energy* **2018**, *155*, 174–189. [CrossRef]

18. Calise, F.; Figaj, R.D.; Vanoli, L. A Novel Polygeneration System Integrating Photovoltaic/Thermal Collectors, Solar Assisted Heat Pump, Adsorption Chiller and Electrical Energy Storage: Dynamic and Energy-Economic Analysis. *Energy Convers. Manag.* **2017**, *149*, 798–814. [CrossRef]

19. Comodi, G.; Giantomassi, A.; Severini, M.; Squartini, S.; Ferracuti, F.; Fonti, A.; Nardi Cesarini, D.; Morodo, M.; Polonara, F. Multi-Apartment Residential Microgrid with Electrical and Thermal Storage Devices: Experimental Analysis and Simulation of Energy Management Strategies. *Appl. Energy* **2015**, *137*, 854–866. [CrossRef]

20. Picallo-Perez, A.; Sala-Lizarraga, J.M. Design and Operation of a Polygeneration System in Spanish Climate Buildings under an Exergetic Perspective. *Energies* **2021**, *14*, 7636. [CrossRef]

21. Ghaem Sigarchian, S.; Malmquist, A.; Martin, V. Design Optimization of a Small-Scale Polygeneration Energy System in Different Climate Zones in Iran. *Energies* **2018**, *11*, 1115. [CrossRef]

22. Experimental Assessment of Thermoelectric Cooling on the Efficiency of PV Module. *Int. J. Renew. Energy Res.* **2022**. [CrossRef]

23. Praveenkumar, S.; Gulakhmadov, A.; Agyekum, E.B.; Alwan, N.T.; Velkin, V.I.; Sharipov, P.; Safaraliev, M.; Chen, X. Experimental Study on Performance Enhancement of a Photovoltaic Module Incorporated with CPU Heat Pipe—A 5E Analysis. *Sensors* **2022**, *22*, 6367. [CrossRef] [PubMed]

24. Stadler, M.; Kloess, M.; Groissböck, M.; Cardoso, G.; Sharma, R.; Bozchalui, M.C.; Marnay, C. Electric Storage in California's Commercial Buildings. *Appl. Energy* **2013**, *104*, 711–722. [CrossRef]

25. Singh, S.; Singh, M.; Kaushik, S.C. Feasibility Study of an Islanded Microgrid in Rural Area Consisting of PV, Wind, Biomass and Battery Energy Storage System. *Energy Convers. Manag.* **2016**, *128*, 178–190. [CrossRef]

26. Destro, N.; Benato, A.; Stoppato, A.; Mirandola, A. Components Design and Daily Operation Optimization of a Hybrid System with Energy Storages. *Energy* **2016**, *117*, 569–577. [CrossRef]

27. Gesteira, L.G.; Uche, J. A Novel Polygeneration System Based on a Solar-Assisted Desiccant Cooling System for Residential Buildings: An Energy and Environmental Analysis. *Sustainability* **2022**, *14*, 3449. [CrossRef]

28. Pina, E.A.; Lozano, M.A.; Serra, L.M. A Multiperiod Multiobjective Framework for the Synthesis of Trigeneration Systems in Tertiary Sector Buildings. *Int. J. Energy Res.* **2019**, *44*, 1140–1166. [CrossRef]

29. *TRNSYS: A Transient System Simulation Program*; Solar Energy Laboratory, University of Wisconsin: Madison, WI, USA, 2006.

30. Duffie, J.A.; Beckman, W.A. *Solar Engineering of Thermal Processes*; John Wiley & Sons: New York, NY, USA, 1991.

31. Eckstein, J.H. Detailed Modeling of Photovoltaic Components. Master's Thesis, University of Wisconsin, Solar Energy Laboratory, Madison, WI, USA, 1990.

32. Buonomano, A.; Calise, F.; Vicidomini, M. Design, Simulation and Experimental Investigation of a Solar System Based on PV Panels and PVT Collectors. *Energies* **2016**, *9*, 497. [CrossRef]

33. Instituto para la Diversificación y Ahorro de la Energia (IDAE). *CO_2 Emission Factors and Primary Energy Coefficients for Different Final Energy Sources Consumed in the Building Sector in Spain*; IDAE: Madrid, Spain, 2014.

34. Spanish Ministry of Development. Updating of the Energy Saving Document DB-HE of the Technical Building Code. 2019. Available online: https://www.codigotecnico.org/pdf/Documentos/HE/DBHE.pdf (accessed on 1 October 2021).

35. Pinto, E.S.; Serra, L.M.; Lázaro, A. Optimization of the Design of Polygeneration Systems for the Residential Sector under Different Self-consumption Regulations. *Int. J. Energy Res.* **2020**, *44*, 11248–11273. [CrossRef]
36. Red Eléctrica Española (REE). *CO₂ Emissions of Electricity Generation in Spain*; REE: Madrid, Spain, 2021.
37. Calise, F.; Cappiello, F.L.; Dentice d'Accadia, M.; Vicidomini, M. Dynamic Simulation, Energy and Economic Comparison between BIPV and BIPVT Collectors Coupled with Micro-Wind Turbines. *Energy* **2020**, *191*, 116439. [CrossRef]
38. Calise, F.; Cappiello, F.L.; Dentice d'Accadia, M.; Petrakopoulou, F.; Vicidomini, M. A Solar-Driven 5th Generation District Heating and Cooling Network with Ground-Source Heat Pumps: A Thermo-Economic Analysis. *Sustain. Cities Soc.* **2022**, *76*, 103438. [CrossRef]
39. Calise, F.; Dentice d'Accadia, M.; Figaj, R.D.; Vanoli, L. A Novel Solar-Assisted Heat Pump Driven by Photovoltaic/Thermal Collectors: Dynamic Simulation and Thermoeconomic Optimization. *Energy* **2016**, *95*, 346–366. [CrossRef]
40. Instituto para la Diversificación y Ahorro de la Energía (IDAE). *Biomass Price Report for Thermal Uses*; IDEA: Madrid, Spain, 2020.
41. Acevedo, L.; Uche, J.; Del Almo, A.; Círez, F.; Usón, S.; Martínez, A.; Guedea, I. Dynamic Simulation of a Trigeneration Scheme for Domestic Purposes Based on Hybrid Techniques. *Energies* **2016**, *9*, 1013. [CrossRef]
42. Angrisani, G.; Roselli, C.; Sasso, M.; Tariello, F. Dynamic Performance Assessment of a Micro-Trigeneration System with a Desiccant-Based Air Handling Unit in Southern Italy Climatic Conditions. *Energy Convers. Manag.* **2014**, *80*, 188–201. [CrossRef]
43. Angrisani, G.; Roselli, C.; Sasso, M. Experimental Assessment of the Energy Performance of a Hybrid Desiccant Cooling System and Comparison with Other Air-Conditioning Technologies. *Appl. Energy* **2015**, *138*, 533–545. [CrossRef]
44. Buonomano, A.; Calise, F.; Ferruzzi, G.; Vanoli, L. A Novel Renewable Polygeneration System for Hospital Buildings: Design, Simulation and Thermo-Economic Optimization. *Appl. Therm. Eng.* **2014**, *67*, 43–60. [CrossRef]
45. Calise, F.; Cappiello, F.L.; Vanoli, R.; Vicidomini, M. Economic Assessment of Renewable Energy Systems Integrating Photovoltaic Panels, Seawater Desalination and Water Storage. *Appl. Energy* **2019**, *253*, 113575. [CrossRef]
46. Mouaky, A.; Rachek, A. Thermodynamic and Thermo-Economic Assessment of a Hybrid Solar/Biomass Polygeneration System under the Semi-Arid Climate Conditions. *Renew. Energy* **2020**, *156*, 14–30. [CrossRef]
47. Uche, J.; Acevedo, L.; Círez, F.; Usón, S.; Martínez-Gracia, A.; Bayod-Rújula, Á.A. Analysis of a Domestic Trigeneration Scheme with Hybrid Renewable Energy Sources and Desalting Techniques. *J. Clean. Prod.* **2019**, *212*, 1409–1422. [CrossRef]
48. Gesteira, L.G.; Uche, J.; de Oliveira Rodrigues, L.K. Residential Sector Energy Demand Estimation for a Single-Family Dwelling: Dynamic Simulation and Energy Analysis. *J. Sustain. Dev. Energy Water Environ. Syst.* **2021**, *9*, 1–18. [CrossRef]
49. Serra, L.M.; Lozano, M.-A.; Ramos, J.; Ensinas, A.V.; Nebra, S.A. Polygeneration and Efficient Use of Natural Resources. *Energy* **2009**, *34*, 575–586. [CrossRef]
50. Wetter, M. GenOpt—A Generic Optimization Program. In Proceedings of the Seventh International IBPSA Conference, Rio de Janeiro, Brazil, 13–15 August 2001; pp. 601–608.
51. Hooke, R.; Jeeves, T.A. "Direct Search" Solution of Numerical and Statistical Problems. *J. ACM* **1961**, *8*, 212–229. [CrossRef]